

# Vacuolar-type proton pump in the basolateral plasma membrane energizes ion uptake in branchial mitochondria-rich cells of killifish *Fundulus heteroclitus*, adapted to a low ion environment

Fumi Katoh\*, Susumu Hyodo and Toyoji Kaneko

Ocean Research Institute, University of Tokyo, 1-15-1 Minamidai, Nakano, Tokyo 164-8639, Japan

\*Author for correspondence (e-mail: fkatoh@ori.u-tokyo.ac.jp)

Accepted 21 November 2002

## Summary

We examined the involvement of mitochondria-rich (MR) cells in ion uptake through gill epithelia in freshwater-adapted killifish *Fundulus heteroclitus*, by morphological observation of MR cells and molecular identification of the vacuolar-type proton pump (V-ATPase). MR cell morphology was compared in fish acclimated to defined freshwaters with different NaCl concentrations: low ( $0.1 \text{ mmol l}^{-1}$ ), mid ( $1 \text{ mmol l}^{-1}$ ) and high ( $10 \text{ mmol l}^{-1}$ )-NaCl environments. MR cells, mostly located on the afferent-vascular side of the gill filaments, were larger in low- and mid-NaCl environments than in the high-NaCl environment. Electron-microscopic observation revealed that the apical membrane of well-developed MR cells in low- and mid-NaCl environments was flat or slightly projecting, and equipped with microvilli to expand the surface area exposed to these environments. On the other hand, in the high-NaCl environment, the apical membrane was invaginated to form a pit, and MR cells often formed multicellular complexes with accessory cells, although the NaCl

concentration was much lower than that in plasma. We cloned and sequenced a cDNA encoding the A-subunit of killifish V-ATPase. The deduced amino acid sequence showed high identity with V-ATPase A-subunits from other vertebrate species. Light-microscopic immunocytochemistry, using a homologous antibody, revealed V-ATPase-immunoreactivity in  $\text{Na}^+/\text{K}^+$ -ATPase-immunoreactive MR cells in low-NaCl freshwater, whereas the immunoreactivity was much weaker in higher NaCl environments. Furthermore, immuno-electron microscopy revealed V-ATPase to be located in the basolateral membrane of MR cells. These findings indicate that MR cells are the site responsible for active ion uptake in freshwater-adapted killifish, and that basolaterally located V-ATPase is involved in the  $\text{Na}^+$  and/or  $\text{Cl}^-$  absorbing mechanism of MR cells.

Key words: mitochondria-rich cell, ion uptake, gill epithelia, freshwater-adapted, killifish, *Fundulus heteroclitus*, V-ATPase.

## Introduction

In teleost fish, plasma osmolality is maintained within a narrow physiological range, equivalent to about one-third seawater osmolality. The gills, kidney and intestine are important osmoregulatory organs in fishes, creating ionic and osmotic gradients between the body fluid and external environments (Evans, 1993). It is well established that gill mitochondria-rich (MR) cells, or chloride cells, are responsible for salt secretion in seawater-adapted fish. In freshwater-adapted teleosts, by contrast, active ion absorption from a hyposmotic environment is necessary to compensate for the constant diffusional loss of ions through the gill epithelia (McCormick, 1995).

The killifish *Fundulus heteroclitus* is a euryhaline species that can be adapted to a wide range of salinities (Griffith, 1974; Hardy, 1978). Killifish branchial MR cells are larger in freshwater than in seawater (Katoh et al., 2001). By contrast, in most fish examined so far, seawater-type MR cells are more

developed in terms of cell size, extension of the tubular system, density of mitochondria and  $\text{Na}^+/\text{K}^+$ -ATPase activity (Langdon and Thorpe, 1985; Richman et al., 1987; McCormick, 1995; Uchida et al., 1996, 2000; Sasai et al., 1998). In freshwater-adapted killifish, the apical membrane of branchial MR cells show projections with microvilli that expand the apical surface area, suggesting active ion absorption through MR cells (Katoh et al., 2001).

The  $\text{Na}^+/\text{H}^+$ -exchanger (NHE) in the apical membrane of gill MR cells has been advocated as the major pathway for  $\text{Na}^+$  uptake and  $\text{H}^+$  excretion in freshwater teleosts. However, it is now considered less likely that  $\text{Na}^+$  uptake occurs *via* NHE, since the driving force for such uptake is lacking in this model (Lin and Randall, 1993). Meanwhile, an alternative model incorporating the vacuolar-type proton pump (V-ATPase) and a conductive  $\text{Na}^+$  channel has been proposed as the  $\text{Na}^+$ -absorbing mechanism. In this model, V-ATPase in the apical

membrane and Na<sup>+</sup>/K<sup>+</sup>-ATPase in the basolateral membrane create the driving force permitting passive electrodiffusion of Na<sup>+</sup> through the Na<sup>+</sup> channel (Avella and Bornancin, 1989). This model has been supported by inhibitory effects of bafilomycin A<sub>1</sub>, a selective inhibitor of V-ATPase, on H<sup>+</sup> secretion and N<sup>+</sup> absorption in frog skins (Klein et al., 1997). Furthermore, Fenwick et al. (1999) reported that bafilomycin A<sub>1</sub> inhibits not only Na<sup>+</sup> but also Cl<sup>-</sup> uptake in gills of tilapia larvae and carp, suggesting a link between Cl<sup>-</sup> uptake and H<sup>+</sup> secretion by V-ATPase.

V-ATPase is one type of ATP-dependent proton pump that is responsible for the acidification of intracellular compartments of eukaryotic cells (Forgac, 1999). V-ATPase also energizes animal plasma membranes (Harvey and Wiczorek, 1997), and is composed of a catalytic V<sub>1</sub> domain responsible for ATP hydrolysis and an integral V<sub>0</sub> domain that forms a channel for H<sup>+</sup> to cross the plasma or vacuolar membranes (Forgac, 1999). Most studies on V-ATPase in fish have been performed in the context of acid-base regulation (Lin et al., 1994; Sullivan et al., 1996; Perry et al., 2000). Although the gills have been identified as the site of V-ATPase activity, the cellular localization of V-ATPase in the gills is still controversial. Immunocytochemical studies with heterologous antibodies have shown that V-ATPase is distributed in both MR and pavement cells in rainbow trout *Oncorhynchus mykiss* (Lin et al., 1994; Wilson et al., 2000a), and in pavement cells but not in MR cells in tilapia *Oreochromis mossambicus* (Hiroi et al., 1998; Wilson et al., 2000a).

In this study, we investigated effects of environmental NaCl concentrations on the morphology and function of gill MR cells in killifish. The MR cell morphology was compared in fish acclimated to defined fresh waters with different NaCl concentrations. Furthermore, to examine the possible involvement of V-ATPase in Na<sup>+</sup> and Cl<sup>-</sup> uptake through gill epithelia, we cloned and sequenced a cDNA encoding the A-subunit of killifish V-ATPase. Using a homologous antibody specific for killifish V-ATPase, we also examined the immunolocalization of V-ATPase in the gill epithelia by light and electron microscopy.

## Materials and methods

### Fish

Experimental fish were the offspring of killifish *Fundulus heteroclitus* L., obtained from the National Research Institute of Fisheries Science, Kanagawa, Japan (Shimizu, 1997). They were reared in seawater at Ocean Research Institute, University of Tokyo, Tokyo, Japan. The fish were kept in a 250 l indoor tank with recirculating seawater at ambient temperature and fed on tilapia pellets (Tilapia 41S, Shikoku Kumiai Shiryō, Japan) once a day. The fish, weighing 7–26 g, were kept in freshwater for 1 month after pre-adaptation to 50% seawater for 1 week. The freshwater-adapted fish were separated into three groups and kept for 1 week in 30 l plastic tanks, which contained defined freshwater + NaCl at different

Table 1. *Environmental ion concentrations used*

	Nominated value (mmol l <sup>-1</sup> )			Measured value (mmol l <sup>-1</sup> )		
	[Na <sup>+</sup> ]	[Cl <sup>-</sup> ]	[Ca <sup>2+</sup> ]	[Na <sup>+</sup> ]	[Cl <sup>-</sup> ]	[Ca <sup>2+</sup> ]
Low-NaCl	0.1	1.1	0.5	0.10	1.40	0.46
Mid-NaCl	1.0	2.0	0.5	0.88	2.20	0.51
High-NaCl	10.0	11.0	0.5	9.92	11.30	0.60

concentrations (low-, mid- and high-NaCl) together with 0.5 mmol l<sup>-1</sup> CaCl<sub>2</sub> (Table 1). The fish were not fed and the water temperature was maintained at 25°C during the experiment.

### Tissue sampling for morphological observations

The fish were anesthetized with 0.05% 2-phenoxyethanol and blood was collected from the caudal vessels into capillary tubes. The plasma was separated by centrifugation at 4000 g for 5 min. Plasma osmolality was measured with a vapor-pressure osmometer (Wascor 5500, UT, USA). Plasma Na<sup>+</sup> concentrations were measured using an atomic absorption spectrophotometer (Hitachi Z-5300, Japan). For the measurement of Na<sup>+</sup>/K<sup>+</sup>-ATPase activity, gill filaments were removed from the gill arch and stored in 200 µl of buffer containing 150 mmol l<sup>-1</sup> sucrose, 10 mmol l<sup>-1</sup> Na<sub>2</sub> EDTA and 50 mmol l<sup>-1</sup> imidazole (SEI buffer) at -80°C until analysis. For whole-mount immunocytochemistry, the gills were removed and fixed in 4% paraformaldehyde (PFA) in 0.1 mol l<sup>-1</sup> phosphate buffer (PB, pH 7.4) for 24 h. For transmission (TEM) and scanning (SEM) electron microscopy, the gills were fixed in 2% PFA–2% glutaraldehyde (GA) in 0.1 mol l<sup>-1</sup> PB for 24 h, postfixed in 1% osmium tetroxide in 0.1 mol l<sup>-1</sup> PB for 1 h, and stored in 70% ethanol. For light- and electron-microscopic immunocytochemistry, the gill filaments were fixed in 2% PFA–0.2% GA in 0.1 mol l<sup>-1</sup> PB for 3 h, and stored in 70% ethanol. For each experimental group, we examined five animals for the whole-mount immunocytochemistry and three for the electron microscopy.

### Measurement of gill Na<sup>+</sup>/K<sup>+</sup>-ATPase activity

Gill Na<sup>+</sup>/K<sup>+</sup>-ATPase activity was measured by a microassay method (Katoh et al., 2001). After 50 µl of SEI buffer containing 0.5% sodium deoxycholic acid was added, the gill filaments stored in 200 µl of SEI buffer were homogenized with a motorized Polytron homogenizer on ice and centrifuged at 3000 g for 10 s to remove insoluble material. The supernatant was assayed for Na<sup>+</sup>/K<sup>+</sup>-ATPase activity and protein content. Homogenate samples (10 µl) were placed in the wells of a 96-well plate in quadruplicate. The assay mixture (200 µl) with or without 0.5 mmol l<sup>-1</sup> ouabain was added to the wells in duplicate just before reading absorbance at a wavelength of 340 nm. The linear rate of NADH disappearance was measured every 2 min up to 10 min. The protein content of the sample was determined using a BCA Protein Assay Kit (Pierce, IL, USA). The Na<sup>+</sup>/K<sup>+</sup>-ATPase activity was calculated as the difference in ATP hydrolysis between the presence

and absence of ouabain, and expressed as  $\mu\text{mol ADP mg protein}^{-1} \text{ h}^{-1}$ .

#### *Molecular identification of the A-subunit of V-ATPase*

The fish acclimated to a low-NaCl environment were anesthetized with 0.05% 2-phenoxyethanol. The gill filaments were dissected out, frozen in liquid N<sub>2</sub>, and stored at  $-80^{\circ}\text{C}$ .

Total RNA was extracted from the gill filaments by the AGPC method described by Chomczynski and Sacchi (1987). Poly(A)<sup>+</sup> RNA purified with Oligotex-dT30 Super (JSR and Nippon Roche, Japan) was treated with the reagents in a Kit (Smart cDNA Library Construction Kit, Clontech Laboratories, CA, USA) to obtain double-stranded cDNAs with 3' and 5' terminal adapters. Polymerase chain reactions (PCRs) were performed using high-fidelity Ex-Taq DNA polymerase (Takara, Japan). The resulting products were ligated into a pT7Blue T-Vector (Novagen, Germany), and then the nucleotide sequences were determined in an automated DNA sequencer (PRISM 310, Perkin-Elmer/Applied Biosystems, CA, USA). The sequences were compared using Genetix-Mac software.

Degenerate PCR primers were designed on the basis of sequences from selected animals (Pan et al., 1991; Graf et al., 1992; Sander et al., 1992; Hille et al., 1993; Hernando et al., 1995; Gill et al., 1998) to obtain a partial cDNA fragment of killifish V-ATPase A-subunit, sense: VATPAf1, GA (A/G) TA(C/T) TT(C/T)(A/C) G (A/C/G/T) GA(C/T) ATGGG; antisense: VATPAR3, CCA (A/G) AA (A/C/G/T) AC(C/T) TG (A/C/G/T) AC (A/G/T) AT (A/C/G/T) CC (Fig. 4). After an initial denaturation at  $96^{\circ}\text{C}$  for 2 min, 30 cycles of PCR were performed, each consisting of 50 s denaturation at  $94^{\circ}\text{C}$ , 30 s annealing at  $50^{\circ}\text{C}$  and 90 s extension at  $72^{\circ}\text{C}$ . Gene-specific primers VATPAf4 and VATPAR1, were designed for the 3'- and 5'-RACE method, respectively: VATPf4, TGGCGGT-GACTTCTCTGACC; and VATPr1, CCAACGCGAGGTG-GAGTCGG (Fig. 4). VATPAf4 and CDS III/3' PCR primer (Smart cDNA Library Construction Kit), and VATPAR1 and 5' PCR primer (Smart cDNA Library Construction Kit) were applied to amplify the 3' and 5' ends, respectively. After a 2 min initial denaturation at  $96^{\circ}\text{C}$ , 35 cycles of PCR were performed as stated above except that the annealing was conducted at  $60^{\circ}\text{C}$ .

To confirm the nucleotide sequence obtained by the 5'- and 3'-RACE method, two gene-specific primers were designed: sense, VATPAf5; CAGCTGACCTCAGCTTACCGTCACG and antisense, VATPAR6; CACACTTGACATTCACC-CACAGAG (Fig. 4). After an initial denaturation at  $96^{\circ}\text{C}$  for 2 min, 35 cycles of the above-mentioned PCR were performed, but the reactions involved 30 s annealing at  $57^{\circ}\text{C}$  and 3 min extension at  $72^{\circ}\text{C}$ .

#### *Antibody*

A polyclonal antiserum was raised in a rabbit against a synthetic peptide based on the highly conserved and hydrophilic region in the A-subunit of V-ATPase. The antigen designed was Cys-Ala-Glu-Met-Pro-Ala-Asp-Ser-Gly-Tyr-

Pro-Ala-Tyr-Leu-Gly-Ala-Arg. The antigen conjugated with keyhole limpet hemocyanin (KLH) was emulsified with complete Freund's adjuvant, and immunization was performed in a New Zealand white rabbit (Sawady Technology, Japan). The antibody was affinity-purified using the synthetic peptide.

#### *Western blot analysis*

The specificity of the raised antibody, named VATP317, was confirmed using western blot analysis. Membrane fractions were prepared from the gills of killifish adapted to low-NaCl freshwater. The gills were homogenized on ice in a buffer consisting of  $25 \text{ mmol l}^{-1}$  Tris-HCl (pH 7.4),  $0.25 \text{ mol l}^{-1}$  sucrose and a pellet ( $50 \text{ ml}^{-1}$ ) of Complete Protein Inhibitor (Boehringer Mannheim, Germany). The homogenate was initially centrifuged at  $4500g$  for 15 min, and the supernatant was subjected to a second centrifugation at  $200000g$  for 1 h. The pellet was resuspended in the same buffer. All the above procedures were performed at  $4^{\circ}\text{C}$ . The protein content of the sample was quantified with a BCA Protein Assay Kit (Pierce). The samples ( $10 \mu\text{g}$ ) were solubilized in a sample-loading buffer, ( $0.25 \text{ mol l}^{-1}$  Tris-HCl, pH 6.8, 2% sodium dodecyl sulfate (SDS), 10%  $\beta$ -mercaptoethanol, 30% glycerol and 0.01% Bromophenol Blue) and heated at  $70^{\circ}\text{C}$  for 15 min. They were separated by SDS-polyacrylamide gel electrophoresis using 7.5% polyacrylamide gels. After electrophoresis, the protein was transferred from the gel to a polyvinylidene difluoride membrane (Atto, Japan).

The membranes were pre-incubated in  $50 \text{ mmol l}^{-1}$  Tris-buffered saline (TBS, pH 7.6) containing 0.05% Triton X-100 and 2% skimmed milk at  $4^{\circ}\text{C}$  overnight, and incubated with the antibody diluted at 1:100 with NB-PBS [ $0.01 \text{ mol l}^{-1}$  phosphate-buffered saline (PBS, pH 7.4) containing 2% normal goat serum (NGS), 0.1% bovine serum albumin (BSA), 0.02% KLH and 0.01% sodium azide] for 1 h at room temperature. The specificity of the immunoreactivity was confirmed by incubating the membranes with the antibody pre-absorbed with the synthetic peptide ( $1 \mu\text{g ml}^{-1}$ ). After rinsing in washing buffer (TBS, 0.05% Triton X-100), the membranes were stained by the avidin-biotin-peroxidase complex (ABC) method, using commercial reagents (Vectastain ABC kit, Vector Laboratories, CA, USA).

#### *Confocal laser scanning microscopy*

For the detection of chloride cells in the whole-mount preparations of the gill filaments, we used an antibody specific for  $\text{Na}^+/\text{K}^+$ -ATPase. The antiserum (NAK121) was raised in a rabbit against a synthetic peptide corresponding to part of the highly conserved region of the  $\text{Na}^+/\text{K}^+$ -ATPase  $\alpha$ -subunit (Katoh et al., 2000), which was based on the method described by Ura et al. (1996). The specific antibody was affinity-purified and labeled with fluorescein isothiocyanate (FITC) as a fluorescent marker. The specificity of the antibody had been confirmed by western blot analysis (Katoh et al., 2000).

The gill filaments were removed from the gill arch prior to the whole-mount immunocytochemistry. After washing in  $0.01 \text{ mol l}^{-1}$  PBS, the whole-mount preparations of the gill

filaments were incubated overnight at 4°C with FITC-labeled NAK121 diluted 1:500 v/v with PBS containing 0.05% Triton X-100, 10% NGS, 0.1% BSA, 0.02% KLH and 0.01% sodium azide. The samples were then washed in PBS for at least 1 h, placed in a chamber slide with a coverslip over, and observed with a confocal laser scanning microscope (LSM 310, Zeiss, Germany). The 488 nm line of an argon-ion laser was used as the excitation wavelength, and the emission was recorded at 515–565 nm.

#### *Quantitative analysis of MR cells*

The size of MR cells stained by the whole-mount immunocytochemistry was measured on stored LSM images by means of an internal program. The MR cell area was obtained from 20 cells per individual ( $N=5$ ), which were randomly selected from gill filaments. For the determination of MR cell density, an area corresponding to 9000–10000  $\mu\text{m}^2$  was randomly selected from the flat region of the afferent-vascular edge, which lacked gill lamellae, of gill filaments in each experimental fish ( $N=5$ ). The MR cells in the selected areas were counted and the density was expressed as cell number per  $\text{mm}^2$ .

#### *Scanning electron microscopy*

The gills fixed for electron microscopy were dehydrated in ethanol, immersed in 2-methyl-2-propanol, and dried using a freeze-drying device (JEOL JFD-300, Japan). Dried samples were mounted on specimen stubs, coated with platinum palladium in an ion sputter (Hitachi E-1030), and examined by SEM (Hitachi S-4500).

#### *Transmission electron microscopy*

After dehydration in ethanol, the gill tissues were transferred to propylene oxide and embedded in Spurr's resin. Ultrathin sections were cut with a diamond knife, mounted on grids, stained with uranyl acetate and lead citrate, and observed with a TEM (Hitachi H-7100).

#### *Immunofluorescence microscopy*

The gill filaments fixed in 2% PFA-0.2% GA in 0.1  $\text{mol l}^{-1}$  PB were immersed in 30% sucrose in 0.01  $\text{mol l}^{-1}$  PBS for 1 h, and embedded in Tissue-Tek OCT compound (Sakura Finetek, Japan) at  $-20^\circ\text{C}$ . Cryosections (2  $\mu\text{m}$ ) were cut on a cryostat (CM 1100, Leica, Germany) at  $-20^\circ\text{C}$ , and collected onto gelatin-coated slides. The compound-removed sections were incubated sequentially with: (1) 2% NGS for 30 min, (2) anti-V-ATPase diluted 1:100 v/v with NB-PBS overnight at 4°C and (3) goat anti-rabbit IgG labeled with Alexa fluor 488 (Molecular Probes, OR, USA) for 2 h at room temperature. To confirm the specificity of the immunoreaction, another cryosection was incubated with the antibody pre-incubated with the synthetic peptide (1  $\mu\text{g ml}^{-1}$ ). These sections were double-stained with the antibody against  $\text{Na}^+/\text{K}^+$ -ATPase (NAK121) labeled with Alexa fluor 546 at a dilution of 1:1000 overnight at 4°C. The sections were observed under a fluorescence microscope (Nikon E800, Japan).

#### *Immuno-electron microscopy*

The gill filaments fixed in 2% PFA-0.2% GA in 0.1  $\text{mol l}^{-1}$  PB were immersed in 30% sucrose in 0.01  $\text{mol l}^{-1}$  PBS for 1 h, and embedded in Tissue-Tek OCT compound (Sakura Finetek) at  $-20^\circ\text{C}$ . Cryosections (16  $\mu\text{m}$ ) were cut on a cryostat (CM 1100, Leica) at  $-20^\circ\text{C}$ , and collected onto gelatin-coated slides. The cryosections were immunocytochemically stained with the antibody against V-ATPase by the ABC method, as described previously. The stained sections were then treated with 1% osmium tetroxide in 0.1  $\text{mol l}^{-1}$  PB for 30 min. After dehydration in ethanol, the sections were transferred to propylene oxide and embedded in Spurr's resin. Ultrathin sections were cut with a diamond knife, and then mounted on grids. These sections were viewed on a TEM (Hitachi H-7100).

#### *Statistics*

All data are presented as the mean  $\pm$  standard error of the mean (S.E.M.). The significance of a difference was determined by Games Howell's test. Before the determinations, analysis of variance (ANOVA) was examined by Bartlett's test.

## **Results**

#### *Plasma osmolality, plasma $\text{Na}^+$ concentration and gill $\text{Na}^+/\text{K}^+$ -ATPase activity*

The plasma osmolality of killifish adapted to defined freshwaters decreased significantly ( $P<0.01$ ) as the environmental NaCl concentration decreased, although the levels stayed within a physiological range (Table 2). The plasma  $\text{Na}^+$  concentration showed a similar pattern to plasma osmolality, with the levels significantly ( $P<0.01$ ) lower in the low-NaCl group than high-NaCl group. Although no significant difference was detected in gill  $\text{Na}^+/\text{K}^+$ -ATPase activity between the three experimental groups, the activity tended to increase with decreasing environmental NaCl concentration (Table 2).

#### *Confocal laser scanning microscopy*

A large number of  $\text{Na}^+/\text{K}^+$ -ATPase-immunoreactive MR cells were detected in the whole-mount preparations of the gill filaments in the three experimental groups (Fig. 1). Immunoreactive MR cells were mostly located in a flat region of the afferent-vascular (trailing) edge of the filament, which lacked gill lamellae, and in the gill filaments between lamellae on the afferent-vascular side. As the environmental NaCl concentration decreased, MR cells extended their distribution toward the efferent side; however, there was no significant difference in MR cell density between three experimental groups (Table 2). Concomitant with the extension of the cell distribution, the cells became significantly larger at lower NaCl concentrations (Table 2).

#### *Scanning electron-microscopic observations*

MR cells were in contact with the external environment through their apical surface. The apical membranes of MR

Table 2. Effects of environmental NaCl concentration on freshwater-adapted killifish

	Low-NaCl	Mid-NaCl	High-NaCl
Osmolality (mOsmol kg <sup>-1</sup> )	303.3±4.7 (10)	330.0±3.4 (9)*	342.0±1.6 (7)*,†
Plasma Na <sup>+</sup> concentration (mmol l <sup>-1</sup> )	159.9±7.4 (9)	175.8±7.5 (9)	195.2±2.4 (7)*
Gill Na <sup>+</sup> , K <sup>+</sup> -ATPase activity (μmol ADP mg protein <sup>-1</sup> h <sup>-1</sup> )	12.1±0.8 (8)	10.6±0.8 (8)	9.0±0.5 (7)
Gill chloride cells			
Size (μm <sup>2</sup> )	201.8±5.9 (5)	117.7±4.2 (5)*	96.5±3.9 (5)*,†
Density (cells mm <sup>-2</sup> )	3374±554 (5)	3774±235 (5)	4329±702 (5)

*N* values are given in parentheses.  
 \**P*<0.01 compared with the low-NaCl group.  
 †*P*<0.01 compared with the mid-NaCl group.

cells were located at the boundary of pavement cells, and most frequently observed on the afferent edge of gill filament epithelia. In low- and mid-NaCl environments, the apical membrane of MR cells did not form a pit, but appeared as a flat or slightly projecting disk among pavement cells (Fig. 2A,C). The apical membrane was equipped with microvilli on its surface (Fig. 2B,D). In the high-NaCl group, in contrast, the apical membrane of most MR cells formed an apical pit, which appeared as a pore among pavement cells (Fig. 2E,F).

#### Transmission electron-microscopic observations

In the three experimental groups, MR cells were generally characterized by a rich population of mitochondria and an extensive tubular system in the cytoplasm (Fig. 3C,F,I). As was seen with SEM, the apical membrane of MR cells was flat or slightly projecting and equipped with numerous microvilli in the low- and mid-NaCl groups (Fig. 3A,B,D,E). In the high-NaCl group, however, the apical membrane of most MR cells was invaginated to form a pit (Fig. 3G,H). Thus, the surface area exposed to ambient water was much larger in fish adapted to lower NaCl environments. In the high-NaCl environment, the MR cells often interdigitated with neighboring accessory cells, forming multicellular complexes. The MR and accessory cells shared an apical pit in the high-NaCl environment, linked by shallow leaky junctions (Fig. 3G,H).

#### V-ATPase A subunit

We cloned and sequenced a full-length cDNA encoding the A-subunit of killifish V-ATPase (2573 bases), and obtained the deduced amino acid sequence (618 amino acids) (Fig. 4). The molecular mass of the killifish V-ATPase A-subunit was estimated to be 68 kDa. The amino acid sequence showed a high degree of identity with V-ATPases from other animal species. The cDNA sequence has been deposited in the DDBJ database with the accession number AB066243.

#### Western blot analysis

The antibody to the V-ATPase A-subunit recognized four protein bands of molecular mass 70–80 kDa (Fig. 5B). However, the two higher protein bands were not affected by pre-incubation of the antibody with the antigen, whereas the lower two bands disappeared when the membrane was incubated with the antigen-absorbed antibody (Fig. 5A). These results indicate that the lower two bands are specific for killifish V-ATPase A-subunit.

#### Immunocytochemical detection of V-ATPase

By immuno-fluorescence microscopy, sagittal sections stained with anti-Na<sup>+</sup>/K<sup>+</sup>-ATPase showed that MR cells were mainly present at the filaments and the base of lamellae (Fig. 6B,D,F,H). Intense V-ATPase-immunoreactivity was detected in Na<sup>+</sup>/K<sup>+</sup>-ATPase-immunoreactive MR cells in the low-NaCl group; the distribution pattern of V-ATPase

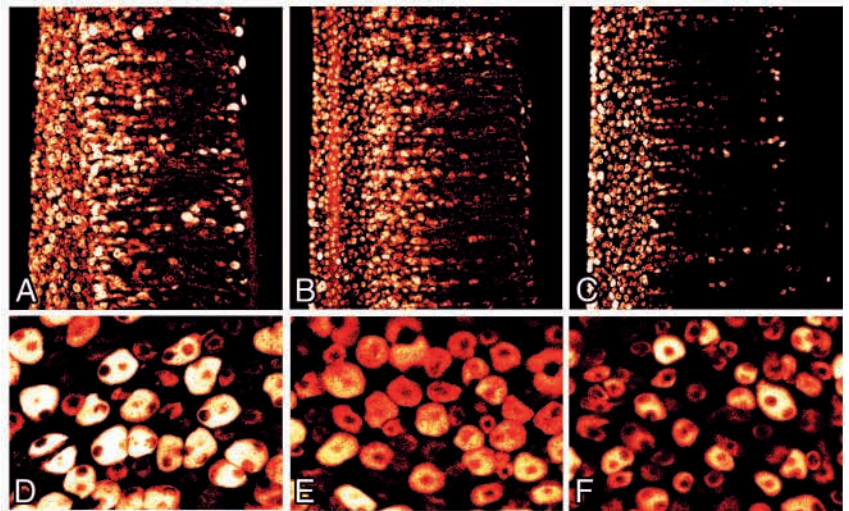


Fig. 1. Confocal laser scanning micrographs of whole-mount preparations of gill filaments in killifish acclimated to defined freshwater with low- (A,D), mid- (B,E) and high- (C,F) NaCl. The gill filaments were stained with FITC-labeled anti-Na<sup>+</sup>, K<sup>+</sup>-ATPase. (D–F) Magnified views of a flat region of the afferent-vascular edge, where most branchial mitochondria-rich (MR) cells are distributed. Scale bars, 100 μm (A–C); 50 μm (D–F).

coincided well with  $\text{Na}^+/\text{K}^+$ -ATPase immunolocalization (Fig. 6A,B). The control procedure in which the specific antibody was pre-incubated with the synthetic peptide resulted in complete extinction of the immunoreactivity (Fig. 6G,H). By contrast, V-ATPase-immunoreactivity in MR cells was much weaker in the mid- and high-NaCl groups than the low-NaCl group (Fig. 6C–F).

The immuno-electron microscopy revealed that V-ATPase was distributed throughout the extensive tubular system, which was continuous with the basolateral membrane of MR cells (Fig. 7). The immunoreaction was detected neither in the apical membrane nor in mitochondria. V-ATPase-immunoreactivity in the basolateral membrane was much

stronger in the low-NaCl group (Fig. 7A,B) than mid-NaCl group (Fig. 7C,D).

### Discussion

In the present study, killifish were well adapted to defined freshwaters with different NaCl concentrations. The plasma osmolality and  $\text{Na}^+$  levels were lowered with decreasing NaCl concentration, but their levels remained within physiological ranges, indicating a successful adaptation to these conditions.

Since  $\text{Na}^+/\text{K}^+$ -ATPase is located in the basolateral membrane of MR cells, the antiserum specific for this enzyme serves as a specific marker for their immunocytochemical detection (Ura et al., 1996). In the present study, MR cells were detected by LSM in the whole-mount preparations of gill filaments, as observed in European sea bass by Varsamos et al. (2002). Although there were no significant differences in the density of MR cells between the three groups, the distribution of MR cells extended toward the efferent-vascular side in lower NaCl environments. Accordingly, the total number of MR cells increased in lower NaCl environments. These results suggest that MR cells in killifish participate in active  $\text{Na}^+$  and/or  $\text{Cl}^-$  absorption from the environment.

Our SEM and TEM observations showed two distinct types of MR cells. When the ambient NaCl concentration was typical of freshwater level or lower (low- and mid-NaCl groups), the apical membrane of MR cells showed slight projections with microvilli. This morphological feature may indicate that killifish MR cells take up ions through the expanded apical surface in lower NaCl environments. A similar structure to the apical membrane has been observed in several species of freshwater-adapted fish (Hossler et al., 1985; Laurent and Hebibi, 1988; Perry et al., 1992; Perry, 1998; Kelly et al., 1999). The apical membrane of MR cells in the high-NaCl group, however, was invaginated to form an apical pit. Furthermore, MR and accessory cells form multicellular complexes, sharing an apical pit. These features are characteristic of MR cells in seawater-adapted fish, and is also the case in killifish (Katoh et al., 2001).

Although ion concentrations in the

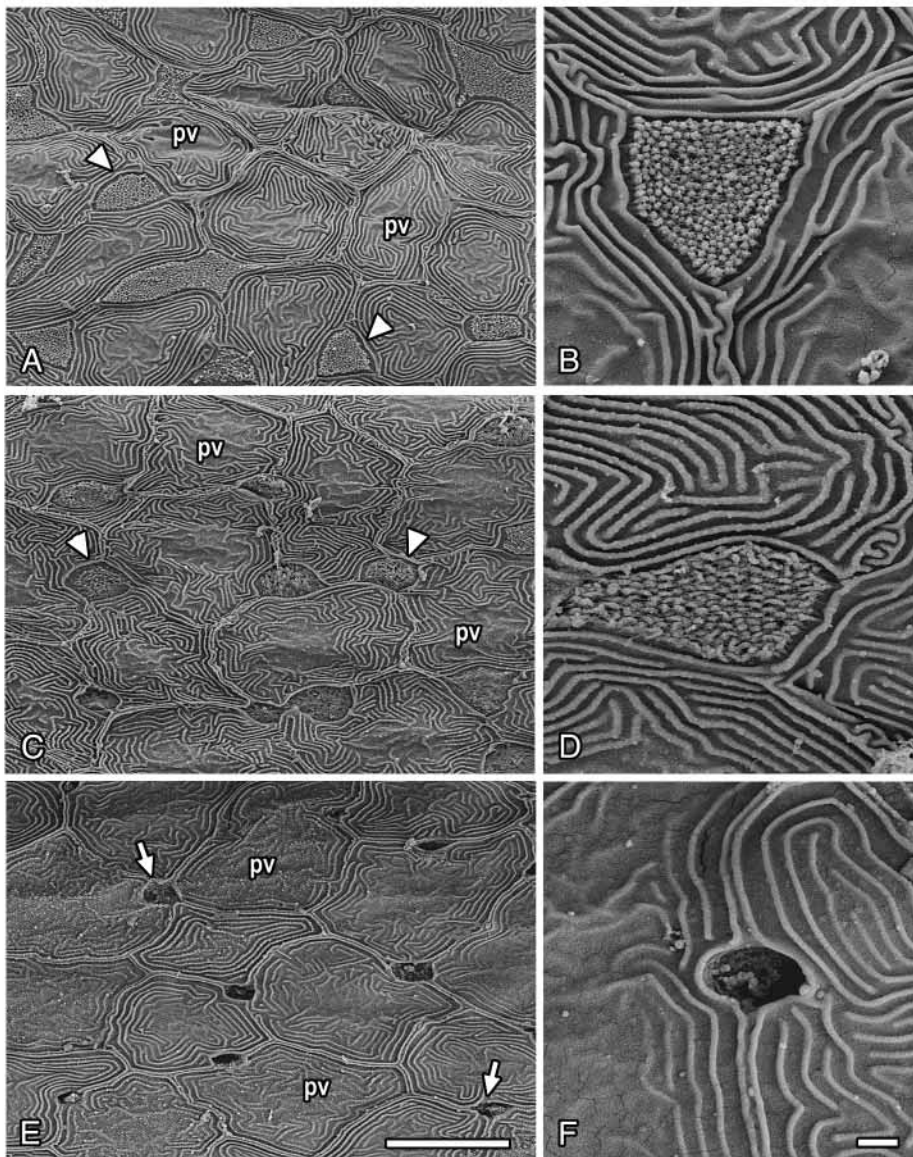


Fig. 2. Scanning electron micrographs of gill filaments in killifish adapted to defined freshwater with low- (A,B), mid- (C,D) and high- (E,F) NaCl. The apical membrane of mitochondria-rich (MR) cells is flat or slightly projecting, and equipped with microvilli (arrowheads) in low- and mid-NaCl groups, whereas the apical membrane of MR cells forms an apical pit (arrows) in the high-NaCl group. pv, pavement cell. Scale bars, 10  $\mu\text{m}$ .

high-NaCl group were much lower than those in seawater, the ultrastructure of MR cells was similar to that observed typically in seawater-adapted fish. Considering the occurrence of seawater- and freshwater-type MR cells in the respective environments (Katoh et al., 2001), the MR cells observed in high-NaCl experimental water might be an intermediate type between seawater and freshwater types. This suggests that the occurrence of two types reflects different functional phases of MR cells. A recent study has demonstrated that freshwater-type MR cells in the yolk-sac membrane of Mozambique tilapia embryos are transformed into seawater-type cells in response to transfer from freshwater to seawater, suggesting plasticity of ion-transporting functions of MR cells (Hiroi et al., 1999). It has been proposed that V-ATPase is involved in ion absorption through gill epithelia in freshwater-adapted fish. In previous studies, antisera raised against mammalian and insect V-ATPases have been applied to immunolocalization of V-ATPase in teleost gills (Lin et al., 1994; Sullivan et al., 1995; Wilson et al., 2000a,b). To obtain more reliable evidence for immunolocalization of V-ATPase, a cDNA encoding the killifish V-ATPase A-subunit was cloned and a specific antibody was raised in this study. The cDNA and deduced amino acid sequences showed high degrees of identity with those of V-ATPase A-subunits from other animals such as bovine (93%, amino acid; 68%, nucleotides; Pan et al., 1991), mouse (93%, 70%; Laitala-Leinonen et al., 1996) and chicken (92%, 68%; Hernando et al., 1995).

In western blot analysis, the antibody recognized two specific protein bands of molecular size approximately 70 kDa, in agreement with the expected size of the killifish V-ATPase A-subunit. It is possible that there exist two V-ATPase A-subunits with different molecular masses in killifish, as is the case in humans (Hille et al., 1993) and chickens (Hernando et al., 1995). The specificity of immunocytochemistry with antibody to V-ATPase was also confirmed; gill MR cells in fish adapted to the low-NaCl environment were intensely stained with the antibody, but the immunoreactivity was extinguished when the antibody had been pre-incubated with the antigen.

The immunoreactivity of V-ATPase was detected in the basolateral membrane of MR cells in the present study, which disagrees with previous observations in teleost gills. In rainbow trout gill epithelia, the V-ATPase is located in the apical membranes of both MR and pavement cells (Perry

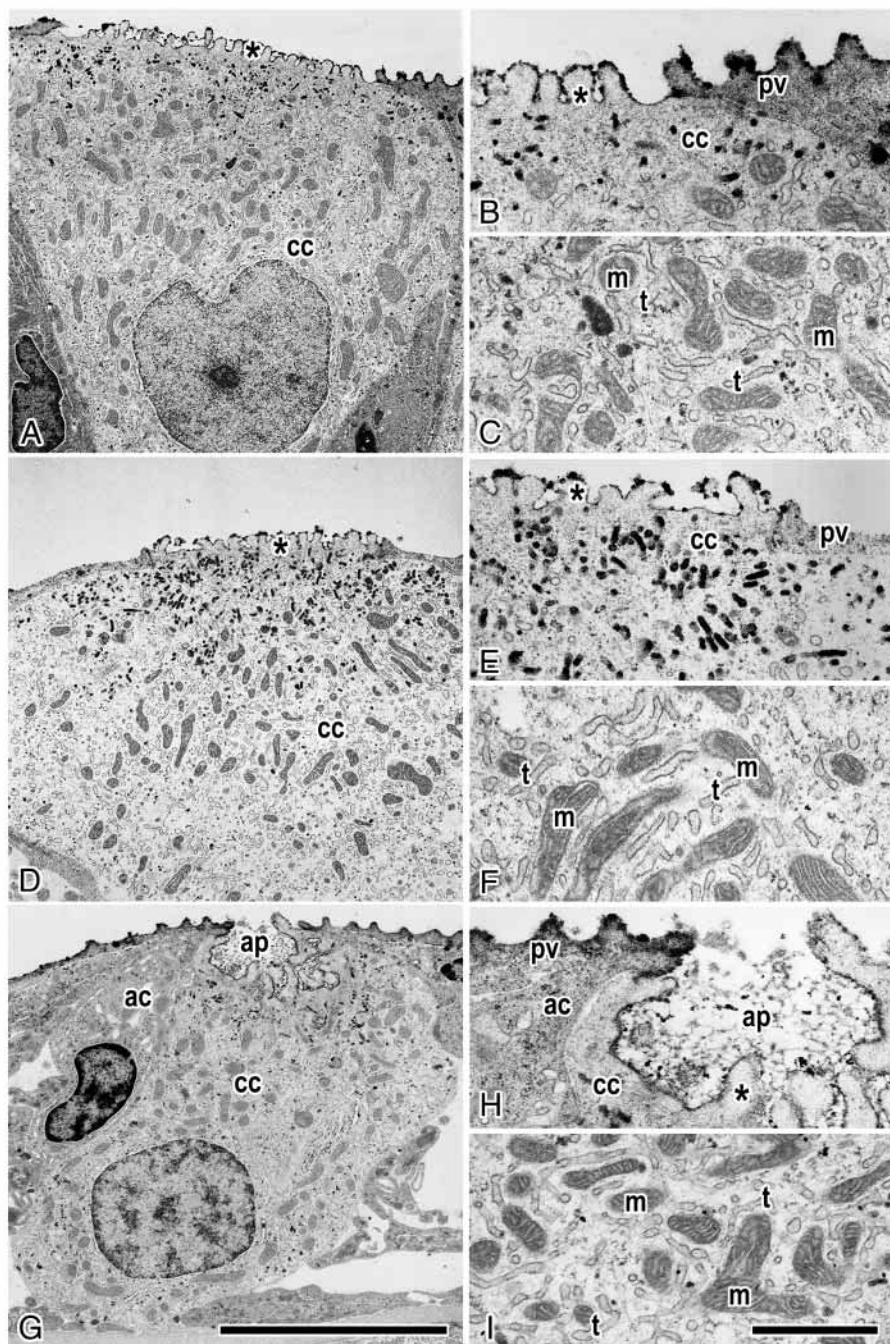


Fig. 3. Transmission electron micrographs of branchial chloride cells (cc) of killifish adapted to defined freshwater with low- (A–C), mid- (D–F) and high- (G–I) NaCl. (B,E,H) Magnified views of apical regions of mitochondria-rich (MR) cells. In low- and mid-NaCl groups, the apical membrane of MR cells is flat or slightly projecting, and equipped with microvilli (asterisks) (B,E). In the high-NaCl group, on the other hand, MR cells form an apical pit (ap) (H). (C,F,I) Magnified views of the cytoplasm of MR cells. Note numerous mitochondria (m) and an extensive tubular system (t) in all experimental groups. pv, pavement cell; ac, accessory cell. Scale bars, 5  $\mu$ m (A,D,G); 1  $\mu$ m (B,C,E,F,H,I).

and Fryer, 1997; Wilson et al., 2000a). V-ATPase immunoreactivity has also been detected in the apical

membrane of lamellar MR cells in mudskipper (Wilson et al., 2000b) and in pavement cells in tilapia (Wilson et al., 2000a).

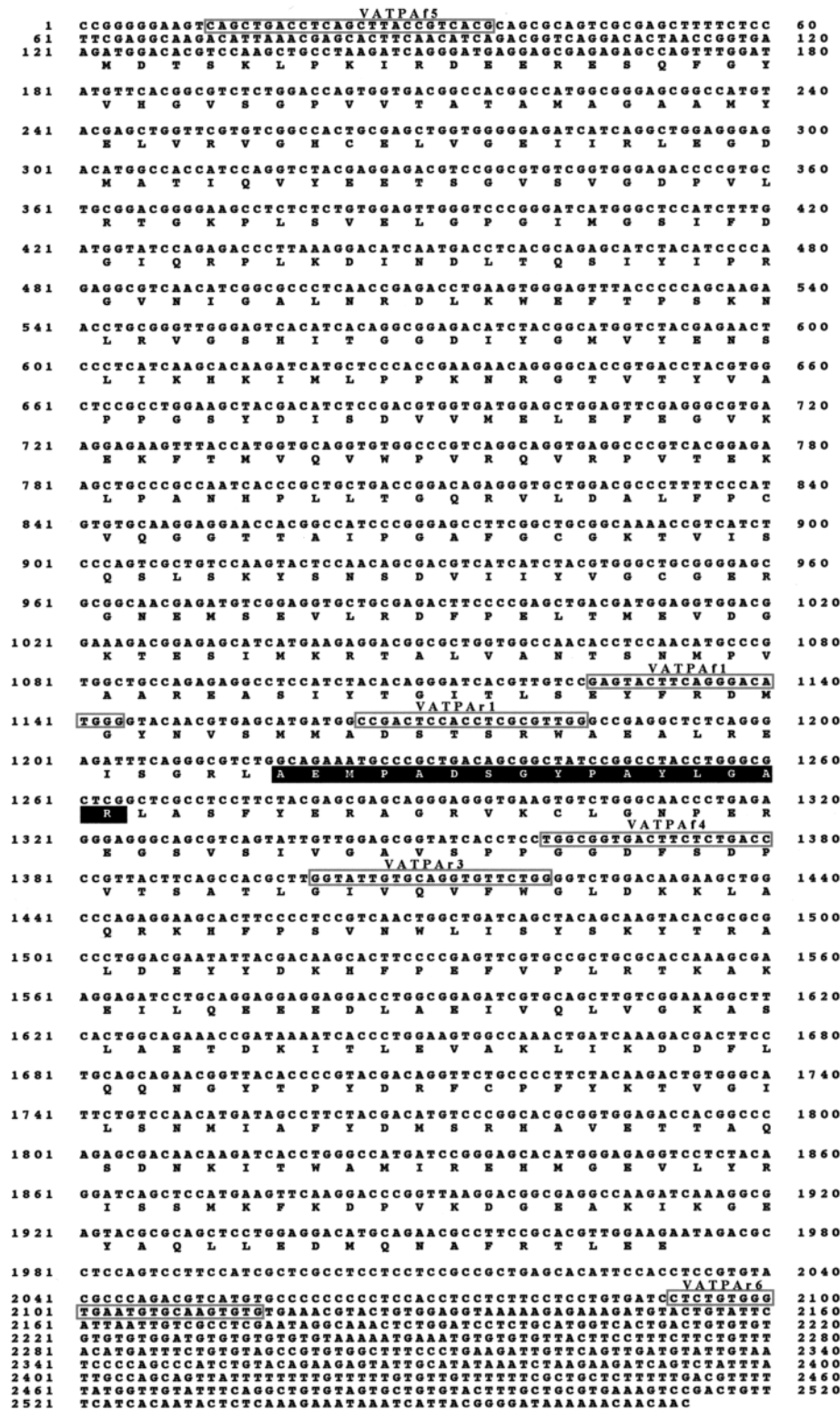


Fig. 4. Nucleotide sequence of the cDNA encoding the A-subunit of the killifish vacuolar-type proton pump and the deduced amino acid sequence. The antibody was raised against a synthetic peptide corresponding to the highlighted amino acid sequence. The sites of PCR primers are shown in the boxes.

In the gills of euryhaline stingray *Dasyatis sabina*, however, the V-ATPase immunoreactivity was detected in the cytoplasm of gill epithelial cells (Piermarini and Evans, 2001), presumably in vesicles or the basolateral membrane, which is in accordance with our observation in killifish. These conflicting results may indicate possible diversity in the distribution and function of V-ATPase in the gill epithelia among different species. A current model in fish gill epithelia and ion-transporting organs of other animal species implicates V-ATPase in both Na<sup>+</sup> and Cl<sup>-</sup> absorption in freshwater. In the mammalian kidney, two subtypes of intercalated cells are present, α- and β-types, which are involved in H<sup>+</sup> and bicarbonate secretion, respectively. V-ATPase is located on the apical plasma membrane in α-cells, and on the basolateral membrane in β-cells. Furthermore, the localization of the Cl<sup>-</sup>/HCO<sub>3</sub><sup>-</sup> anion exchanger (band 3) has been demonstrated on the basolateral membrane in α-cells and on the apical membrane in β-cells (Brown and

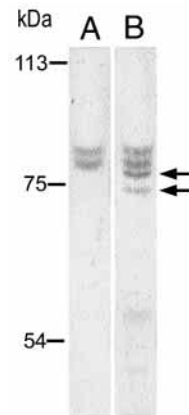
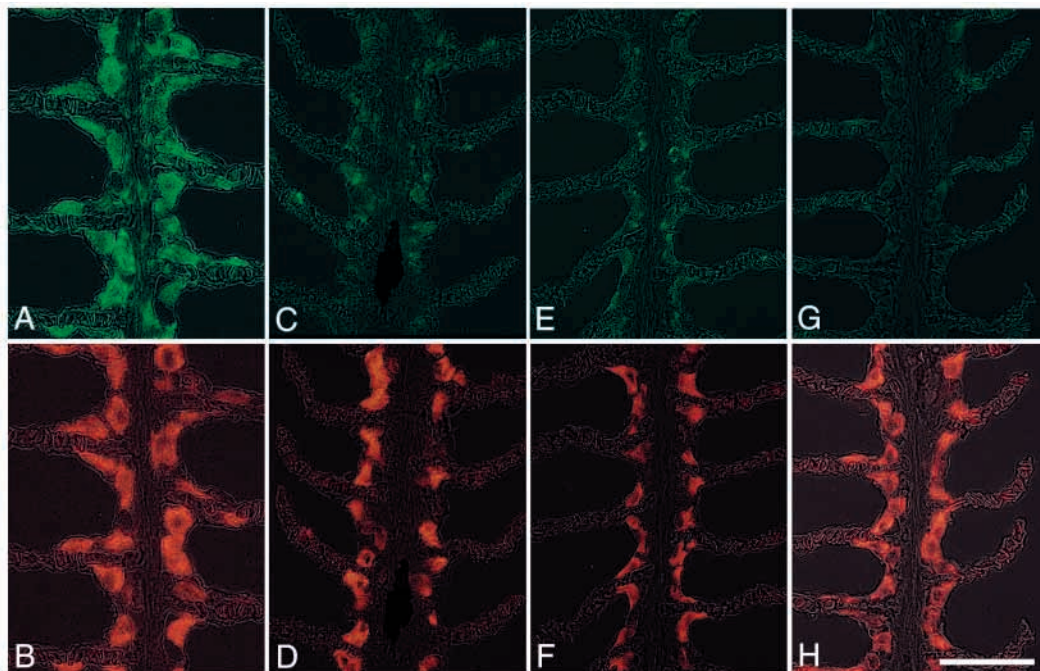


Fig. 5. Western blot analysis for vacuolar-type proton pump (V-ATPase) protein expressed in the gills of killifish adapted to a low-NaCl environment. The membranes were incubated with anti-V-ATPase (lane B) and antibody pre-incubated with the antigen (lane A). Positions of molecular markers (kDa) are indicated on the left side of the figure. Two specific protein bands (arrows) were obtained.

Fig. 6. Double immunofluorescence staining of the vacuolar-type proton pump (V-ATPase: A,C,E,G) and  $\text{Na}^+/\text{K}^+$ -ATPase (B,D,F,H) in the gill filaments of killifish adapted to freshwater with low- (A,B,G,H), mid- (C,D) and high- (E,F) NaCl. V-ATPase immunoreactivity was detected in  $\text{Na}^+/\text{K}^+$ -ATPase-immunoreactive mitochondria-rich (MR) cells in fish adapted to a low-NaCl environment (A,B), but the staining was extinguished when antibody was pre-absorbed with the antigen (G). V-ATPase-immunoreactivity was faint in higher NaCl environments (C,E). Scale bar, 50  $\mu\text{m}$ .



Breton, 1996, 2000). In these intercalated cells, carbonic anhydrase II catalyzes the dehydration of  $\text{CO}_2$  to produce  $\text{H}^+$  and  $\text{HCO}_3^-$ . In euryhaline stingray, pendrin (a kind of anion exchanger) immunoreactivity occurred on the apical region of cells rich in basolateral V-ATPase (Piermarini et al., 2002). In the present study, V-ATPase was detected in the basolateral membrane of branchial MR cells, as was seen in mammalian  $\beta$ -type intercalated cells and branchial cells of stingray. It is thus possible that  $\text{H}^+$  transport from the MR cell to blood by V-ATPase facilitates  $\text{Cl}^-$  absorption through the apically located anion exchanger. In the present study, however, the  $\text{Na}^+$  concentration was much lower than that in normal fresh water in the low-NaCl group (Table 1), where V-ATPase was intensely expressed in MR cells. Accordingly, it is more likely that the MR cell development and expression of V-ATPase in the basolateral membrane are attributable to a low  $\text{Na}^+$  concentration, rather than a low  $\text{Cl}^-$  concentration. In freshwater-adapted fish, NHE has been considered one possible pathway for  $\text{Na}^+$  uptake through gill epithelia (McCormick, 1995); however, there is no logical explanation of the driving force for NHE (Lin and Randall, 1995). The  $\text{Na}^+$  gradient between the surrounding water and epithelial cells could be the driving force for  $\text{Na}^+$  uptake; however,  $\text{Na}^+$  concentrations in the gill epithelial cells should be much higher than those in fresh water. Using a fluorescent  $\text{Na}^+$  indicator, Li et al. (1997) estimated  $\text{Na}^+$  concentration in the cytoplasm of the gill epithelial cells to be approximately  $12 \text{ mmol l}^{-1}$ . Thus, the  $\text{Na}^+$  gradient across the apical membrane could not possibly drive NHE (Avella and Bornancin, 1989). By contrast, V-ATPase coupled with an amiloride-sensitive  $\text{Na}^+$  channel, another possible pathway for  $\text{Na}^+$  uptake, is plausible because the driving force for  $\text{Na}^+$  uptake can be created by ATPase.

The model of  $\text{Na}^+$  uptake by V-ATPase coupled with the amiloride-sensitive  $\text{Na}^+$  channel has been well described in frog skin, in which V-ATPase is located in the apical membrane of MR cells. In a freshwater environment ( $1 \text{ mmol l}^{-1} \text{ Na}_2\text{SO}_4$ ), bafilomycin  $\text{A}_1$  ( $10 \mu\text{mol l}^{-1}$ ) blocked  $\text{H}^+$  excretion and therefore  $\text{Na}^+$  absorption in open-circuited skins (Klein et al., 1997). In recent studies, it has also been reported that bafilomycin  $\text{A}_1$  reduces whole-body  $\text{Na}^+$  influx in tilapia larvae and carp fry (Fenwick et al., 1999), supporting this model in fish species. Li et al. (1997) also revealed that amiloride and tetrodotoxin inhibit  $\text{Na}^+$  flux in MR cells isolated from Mozambique tilapia.

Based on our observations that  $\text{Na}^+/\text{K}^+$ -ATPase and V-ATPase are co-localized in the basolateral membrane in killifish gill MR cells, we propose another model for  $\text{Na}^+$  uptake through gill MR cells in freshwater-adapted killifish. When basolaterally located  $\text{Na}^+/\text{K}^+$ -ATPase and V-ATPase transport  $\text{Na}^+$  and  $\text{H}^+$ , respectively, from MR cells to blood, the MR cells would be negatively charged. According to the electrical gradient established by  $\text{Na}^+/\text{K}^+$ -ATPase and V-ATPase,  $\text{Na}^+$  is absorbed *via* apically located  $\text{Na}^+$  channels. Actually, in the granular cells of frog, another cell type in frog skin epithelia, it is supposed that  $\text{Na}^+$  is absorbed by the electrical gradient created by  $\text{Na}^+/\text{K}^+$ -ATPase located in the basolateral membrane (Ehrenfeld and Klein, 1997). In killifish, V-ATPase facilitated the creation of a steeper electrical gradient in collaboration with  $\text{Na}^+/\text{K}^+$ -ATPase for absorption of  $\text{Na}^+$  from low  $\text{Na}^+$  environments. This may explain why V-ATPase was intensely expressed in the extremely low  $\text{Na}^+$  environment.

Wilson et al. (2000a) examined the immunolocalization of  $\text{Na}^+$  channels using an antibody to the  $\beta$ -subunit of human epithelial  $\text{Na}^+$  channels. They reported that  $\text{Na}^+$  channel and

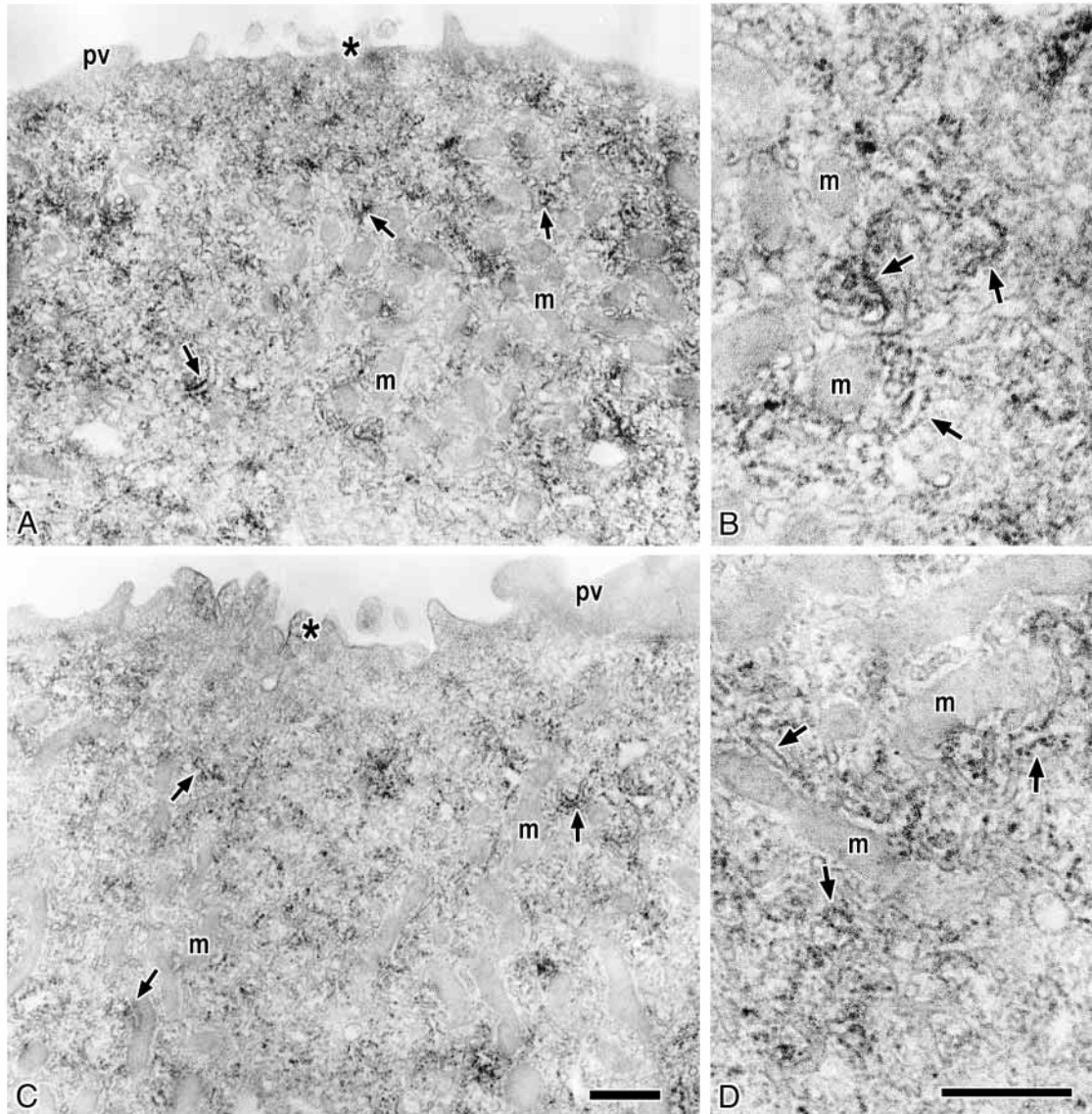


Fig. 7. Immuno-electron micrographs of the vacuolar-type proton pump (V-ATPase) in gill chloride cells of killifish adapted to low-NaCl (A,B) and mid-NaCl (C,D). V-ATPase immunoreactivity was detected in the tubular system (arrows) continuous with the basolateral membrane, but not in the apical membrane (asterisks) and mitochondria (m) in mitochondria-rich (MR) cells (A,C). (B,D) Magnified views of the cytoplasm in MR cells. The staining was more intense in the low-NaCl environment than in the mid-NaCl environment. pv, pavement cell. Scale bars, 1  $\mu\text{m}$  (A,C); 0.5  $\mu\text{m}$  (B,D).

V-ATPase immunoreactivities were co-localized in pavement cells in freshwater tilapia and rainbow trout, although the apical labeling of  $\text{Na}^+$  channels was also found in MR cells in rainbow trout. The localization of  $\text{Na}^+$  channels was not addressed in the present study; however, it is highly possible that the  $\text{Na}^+$  channel is located in the apical membrane of MR cells in killifish.

We express our gratitude to Prof. Greg G. Goss, University of Alberta, for critical reading of the manuscript. We thank Dr Akio Shimizu, National Research Institute of Fisheries Science, for supplying us with the killifish. This study was supported in part by a Grant-in-Aid for Scientific Research

from the Ministry of Education, Culture, Sports, Science and Technology, Japan. F.K. was supported by a Research Fellowship awarded by the Japan Society for the Promotion of Science for Young Scientists.

### References

- Avella, M. and Bornancin, M. (1989). A new analysis of ammonia and sodium transport through the gills of the freshwater rainbow trout (*Salmo gairdneri*). *J. Exp. Biol.* **142**, 155-175.
- Brown, D. and Breton, S. (1996). Mitochondria-rich, proton-secreting epithelial cells. *J. Exp. Biol.* **199**, 2345-2358.
- Brown, D. and Breton, S. (2000).  $\text{H}^+$  V-ATPase-dependent luminal acidification in the kidney collecting duct and the epididymis/vas deferens: vesicle recycling and transcytotic pathway. *J. Exp. Biol.* **203**, 137-145.

- Chomczynski, P. and Sacchi, N. (1987). Single-step of RNA isolation by acid guanidinium thiocyanate-phenol-chloroform extraction. *Anal. Biochem.* **163**, 156-159.
- Ehrenfeld, J. and Klein, U. (1997). The key role of the H<sup>+</sup> V-ATPase in acid-base balance and Na<sup>+</sup> transport process in frog skin. *J. Exp. Biol.* **200**, 247-256.
- Evans, D. H. (1993). Osmotic and ionic regulation. In *The Physiology of Fishes* (ed. D. H. Evans), pp. 315-341. Boca Raton, FL: CRC Press.
- Fenwick, J. C., Wendelaar Bonga, S. E. and Flik, G. (1999). *In vivo* bafilomycin-sensitive Na<sup>+</sup> uptake in young freshwater fish. *J. Exp. Biol.* **202**, 3659-3666.
- Forgac, M. (1999). Structure and properties of the vacuolar (H<sup>+</sup>)-ATPases. *J. Biol. Chem.* **274**, 12951-12954.
- Gill, S. S., Chu, P. B., Smethurst, P., Pietrantonio, P. V. and Ross, L. S. (1998). Isolation of the V-ATPase A and c subunit cDNAs from mosquito midgut and malpighian tubules. *Arch. Insect. Biochem. Physiol.* **37**, 80-90.
- Graf, R., Novak, F. J., Harvey, W. R. and Wiczorek, H. (1992). Cloning and sequencing of cDNA encoding the putative insect plasma membrane V-ATPase subunit A. *FEBS Lett.* **300**, 119-122.
- Griffith, R. W. (1974). Environment and salinity tolerance in the genus *Fundulus*. *Copeia* **1974**, 319-331.
- Hardy, J. D., Jr (1978). *Development of Fishes of Mid-Atlantic Bight*, vol. 2. Washington, DC: Government Printing Office.
- Harvey, W. R. and Wiczorek, H. (1997). Animal plasma membrane energization by chemiosmotic H<sup>+</sup> V-ATPase. *J. Exp. Biol.* **200**, 203-216.
- Hernando, N., Bartkiewicz, M., Collin-Osdoby, P., Osdoby, P. and Barton, R. (1995). Alternative splicing generates a second isoform of the catalytic A subunit of the vacuolar H<sup>+</sup>-ATPase. *Proc. Natl. Acad. Sci. USA* **92**, 6087-6091.
- Hille, B. V., Richener, H., Evans, D. B., Green, J. R. and Bilbe, G. (1993). Identification of two subunit A isoforms of the vacuolar H<sup>+</sup>-ATPase in human osteoclastoma. *J. Biol. Chem.* **268**, 7075-7080.
- Hiroi, J., Kaneko, T., Uchida, K., Hasegawa, S. and Tanaka, M. (1998). Immunolocalization of vacuolar-type H<sup>+</sup>-ATPase in the yolk-sac membrane of tilapia (*Oreochromis mossambicus*) larvae. *Zool. Sci.* **15**, 447-453.
- Hiroi, J., Kaneko, T. and Tanaka, M. (1999). *In vivo* sequential changes in chloride cell morphology in the yolk-sac membrane of Mozambique tilapia (*Oreochromis mossambicus*) embryos and larvae during seawater adaptation. *J. Exp. Biol.* **202**, 3485-3495.
- Hossler, F. E., Musil, G., Karnaky, K. J., Jr and Epstein, F. H. (1985). Surface structure of the gill arch of the killifish, *Fundulus heteroclitus*, from seawater and freshwater, with special reference to the morphology of apical crypt of chloride cells. *J. Morphol.* **185**, 377-386.
- Katoh, F., Shimizu, A., Uchida, K. and Kaneko, T. (2000). Shift of chloride cell distribution during early life stages in seawater-adapted killifish, *Fundulus heteroclitus*. *Zool. Sci.* **17**, 11-18.
- Katoh, F., Hasegawa, S., Kita, J., Takagi, Y. and Kaneko, T. (2001). Distinct seawater and freshwater types of chloride cells in killifish, *Fundulus heteroclitus*. *Can. J. Zool.* **79**, 822-829.
- Kelly, S. P., Chow, I. N. K. and Woo, N. Y. S. (1999). Haloplasticity of black seabream (*Mylio macrocephalus*): hypersaline of freshwater acclimation. *J. Exp. Zool.* **283**, 226-241.
- Klein, U., Timme, M., Zeiske, W. and Ehrenfeld, J. (1997). The H<sup>+</sup> pump in frog skin (*Rana esculenta*): Identification and localization of a V-ATPase. *J. Membr. Biol.* **157**, 117-126.
- Laitala-Leinonen, T., Howell, M. L., Dean, G. E. and Vaananen, H. K. (1996). Resorption-cycle-dependent polarization of mRNAs for different subunits of V-ATPase in bone-resorbing osteoclasts. *Mol. Biol. Cell* **7**, 129-142.
- Langdon, J. S. and Thorpe, J. E. (1985). The ontogeny of smoltification: developmental patterns of gill Na<sup>+</sup>, K<sup>+</sup>-ATPase, SDH and chloride cells in juvenile Atlantic salmon *Salmo Salar* L. *Aquaculture*. **45**, 83-95.
- Laurent, P. and Hebibi, N. (1988). Gill morphology and osmoregulation. *Can. J. Zool.* **67**, 3055-3063.
- Li, J., Eygensteyn, J., Lock, B. A. C., Wendelaar Bonga, S. E. and Flik, G. (1997). Na<sup>+</sup> and Ca<sup>2+</sup> homeostatic mechanisms in isolated chloride cells of the teleost *Oreochromis mossambicus* analyzed by confocal laser scanning microscopy. *J. Exp. Biol.* **200**, 1499-1508.
- Lin, H. and Randall, D. J. (1993). H<sup>+</sup>-ATPase activity in crude homogenates of fish gill tissue: inhibitor sensitivity and environmental and hormonal regulation. *J. Exp. Biol.* **180**, 163-174.
- Lin, H., Pfeiffer, D. C., Vogl, A. W., Pan J. and Randall, D. J. (1994). Immunolocalization of H<sup>+</sup>-ATPase in the gill epithelia of rainbow trout. *J. Exp. Biol.* **195**, 169-183.
- Lin, H. and Randall, D. J. (1995). Proton pumps in fish gills. In *Cellular and Molecular Approaches to Fish Ionic Regulation* (ed. C. M. Wood and T. J. Shuttleworth), pp. 229-255. New York: Academic Press.
- McCormick, S. D. (1995). Hormonal control of gill Na<sup>+</sup>, K<sup>+</sup>-ATPase and chloride cell function. In *Cellular and Molecular Approaches to Fish Ionic Regulation* (ed. C. M. Wood and T. J. Shuttleworth), pp. 285-315. New York: Academic Press.
- Pan, Y. X., Xu, J., Strasser, J. E., Howell, M. and Dean, G. E. (1991). Structure and expression of subunit A from the bovine chromaffin cell vacuolar ATPase. *FEBS Lett.* **293**, 89-92.
- Perry, S. F., Goss, G. G. and Laurent, P. (1992). The interrelationships between gill chloride cell morphology and ionic uptake in four freshwater teleosts. *Can. J. Zool.* **70**, 1775-1786.
- Perry, S. F. and Fryer, J. N. (1997). Proton pumps in the fish gill and kidney. *Fish Physiol. Biochem.* **17**, 363-369.
- Perry, S. F. (1998). Relationship between branchial chloride cells and gas transfer in freshwater fish. *Comp. Biochem. Physiol. A* **119**, 9-16.
- Perry, S. F., Matthew, L. B. and Johnson, D. A. (2000). Cloning and molecular characterization of the trout (*Oncorhynchus mykiss*) vacuolar H<sup>+</sup>-ATPase B subunit. *J. Exp. Biol.* **203**, 459-470.
- Piermarini, P. M. and Evans, D. H. (2001). Immunohistochemical analysis of the vacuolar proton-ATPase B-subunit in the gills of a euryhaline stingray (*Dasyatis sabina*): effects of salinity and relation to Na<sup>+</sup>/K<sup>+</sup>-ATPase. *J. Exp. Biol.* **204**, 3251-3259.
- Piermarini, P. M., Verlander, J. W., Royaux, I. E. and Evans, D. H. (2002). Pendlin immunoreactivity in the gill epithelium of a euryhaline elasmobranch. *Am. J. Physiol.* **283**, R983-R992.
- Richman, N. H., Tai de Dais, S., Nishioka, R. S., Prunet, P. and Bern, H. A. (1987). Osmoregulatory and endocrine relationships with chloride cell morphology and density during smoltification in coho salmon (*Oncorhynchus kisutch*). *Aquaculture* **135**, 185-193.
- Sander, I., Lottspeich, F., Appelhans, H., Kojro, E., Spangenberg, J., Weindel, C., Haase, W. and Koepsell, H. (1992). Sequence analysis of the catalytic subunit of H<sup>+</sup>-ATPase from porcine renal brush-border membrane. *Biochem. Biophys. Acta* **1112**, 129-141.
- Sasai, S., Kaneko, T., Hasegawa, S. and Tsukamoto, K. (1998). Morphological alternation in two types of gill chloride cells in Japanese eel (*Anguilla japonica*) during catadromous migration. *Can. J. Zool.* **76**, 1480-1487.
- Shimizu, A. (1997). Reproductive cycles in a reared strain of the mummichog, a daily spawner. *J. Fish. Biol.* **51**, 724-737.
- Sullivan, G. V., Fryer, J. N. and Perry, S. F. (1995). Immunolocalization of proton pumps (H<sup>+</sup>-ATPase) in pavement cells of rainbow trout gill. *J. Exp. Biol.* **198**, 2619-2629.
- Sullivan, G. V., Fryer, J. N. and Perry, S. F. (1996). Localization of mRNA for the proton pump (H<sup>+</sup>-ATPase) and Cl<sup>-</sup>/HCO<sub>3</sub><sup>-</sup> exchanger in the rainbow trout gill. *Can. J. Zool.* **74**, 2095-2103.
- Uchida, K., Kaneko, T., Yamauchi, K. and Hirano, T. (1996). Morphometrical analysis of chloride cell activity in the filaments and lamellae and changes in Na<sup>+</sup>, K<sup>+</sup>-ATPase activity during seawater adaptation in chum salmon fry. *J. Exp. Zool.* **276**, 193-200.
- Uchida, K., Kaneko, T., Miyazaki, H., Hasegawa, S. and Hirano, T. (2000). Excellent salinity tolerance of Mozambique tilapia (*Oreochromis mossambicus*): elevated chloride cell activity in the branchial and opercular epithelia of the fish adapted to concentrated seawater. *Zool. Sci.* **17**, 149-160.
- Ura, K., Soyano, K., Omoto, N., Adachi, S. and Yamauchi, K. (1996). Localization of Na<sup>+</sup>, K<sup>+</sup>-ATPase in tissues of rabbit and teleosts using an antiserum detected against a partial sequence of the  $\alpha$ -subunit. *Zool. Sci.* **13**, 219-277.
- Varsamos, S., Daiz, J. P., Charmantier, G., Blasco, C., Connors, R. and Flik, G. (2002). Localization and morphology of chloride cells during the post-embryonic development of the European sea bass, *Dicentrarchus labrax*. *Anat. Embryol.* **205**, 203-213.
- Wilson, J. M., Laurent, P., Tufts, B., Benos, D. J., Donowitz, M., Vogl, A. W. and Randall, D. J. (2000a). NaCl uptake by the branchial epithelium in freshwater teleost fish: an immunological approach to ion-transport protein localization. *J. Exp. Biol.* **203**, 2279-2296.
- Wilson, J. M., Randall D. J., Donowitz, M., Wayne Vogl, A. and Alex, K. Y. I. P. (2000b). Immunolocalization of ion-transport proteins to branchial epithelium mitochondria-rich cells in the mudskipper (*Periophthalmodon schlosseri*). *J. Exp. Biol.* **203**, 2297-2310.